*Solid State Phenomena*
*ISSN: 1662-9779, Vol. 373, pp 39-48*
*doi:10.4028/p-Sa2SMr*

*Submitted: 2024-08-09*
*Revised: 2025-04-25*
*Accepted: 2025-04-29*
*Online: 2025-07-18*

# Spin-Polarized Positron Annihilation Spectroscopy -Principles and Applications in Materials Study-

A. Kawasuso

National Institute for Quantum Science and Technology, 1233, Watanuki, Takasaki, Gunma, 370-1292, Japan

kawasuso.atsuo@qst.go.jp

**Keywords:** Positron, Beam, Spin, Ferromagnet, Spintronics

**Abstract.** In the summer school of PSD2024, focusing on spin-polarized positron annihilation spectroscopy in materials science, I reported the historical background and its possibility concerning current spintronics field, the basic principles, and prospects. Here, as a memorandum, I mainly summarize the basic principles, which can be relatively well-formulated, with some remarks.

## History and Current Motivation

In 1956, Yang and Lee proposed the need for some experimentation to confirm parity violation in the weak interaction, given the lack of evidence of parity conservation [1]. In 1957, Wu and her collaborators demonstrated that parity is broken in the $\beta^-$ decay of $^{60}$Co radioisotopes [2]. If this is true, then the electrons/positrons emitted in β decay should be longitudinally spin-polarized. After Wu, Hanna and Preston showed spin polarization of positrons in $^{64}$Cu radioisotopes [3]. As a result, a study of ferromagnetic band structure using spin-polarized positrons and angular correlation of annihilation radiation (ACAR) spectroscopy was initiated [4,5]. This is the prototype of spin-polarized positron annihilation spectroscopy (SP-PAS). In 1979, a spin-polarized positron beam was developed [6]. At that time, surface physics was in a period of rapid development. The so-called magnetic dead layer hypothesis was proposed in this context. [7]. Contrary to this expectation, the SP-PAS study showed that the top surface of ferromagnetic Ni is in the magnetically living layer and not in the dead layer. [8]. In 1987, the spin relaxation effect of positrons in diffusion process was studied using ferromagnetic Fe. [9]. To date, SP-PAS has been used to study magnetic systems.

Today, the research field of spintronics has emerged to solve problems in electronic devices such as energy consumption and performance limitations [10]. New concepts and principles found in the fundamental solid-state physics, such as the novel spin phenomena occurring at the surface and interface [11] and the discovery of a new class of topological materials [12, 13] would be the foundation of next technological innovation. A vast array of materials and phenomena have been extensively studied in relation to the generation, manipulation, and transport of spin [14]. Unprecedented experimental tools are always needed to reveal hidden new aspects of materials.

SP-PAS can respond to this offer because it can selectively detect electron spins at different locations in the material, i.e., top-surface, interface, deep in the bulk, and atomic vacancies. The basic principles of this approach are summarized below.

## Basic Principles

### (i) Parity violation in the weak interaction

$\beta^+$ decay involves the conversion of proton to neutron, and the emissions of positron ($e^+$) and electron neutrino ($\nu_e$). The term of weak interaction is because this reaction is mediated by weak boson. Both positron and electron neutrino have spin 1/2 and hence the change in the nuclear spin after the decay is –1. Positron and electron neutrino are emitted into a mutually opposite $\pi$-direction parallel to the nuclear spin. In this case, as shown in Fig. 1, parity-transformed two processes, i.e., positron with positive (negative) helicity and electron neutrino with negative (positive) helicity may be possible. However, electron neutrino can take only negative helicity and only the upper emission type in Fig.

1 is allowed. This is the parity violation and hence positrons are naturally and longitudinally spin-polarized. Spin polarization is given by the helicity itself, $v/c$, where $v$ and $c$ are the velocities of positron and light, respectively.

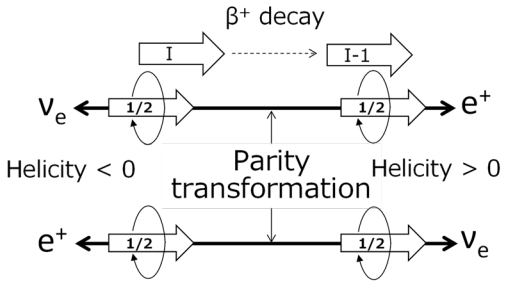


**Fig. 1** Relationship between nuclear spin and motions of positron and electron neutrino in $\beta^+$-decay.

**Table 1** Characteristics of various positron sources. $E_{max}$, and <E> are the endpoint and mean energies of positron.

| Isotope | Half-life | $E_{max}$ / MeV | <E> / MeV | <v>/c |
|---|---|---|---|---|
| $^{18}$F | 110 m | 0.63 | 0.26 | 0.75 |
| $^{22}$Na | 2.6 y | 0.55 | 0.22 | 0.72 |
| $^{26}$Al | 740000 y | 1.17 | 0.55 | 0.88 |
| $^{27}$Si | 4.2 s | 3.79 | 2.60 | 0.99 |
| $^{44}$Ti-$^{44}$Sc | 49 y | 1.47 | 0.64 | 0.90 |
| $^{64}$Cu | 12.7 h | 0.65 | 0.28 | 0.76 |
| $^{58}$Co | 70.8 d | 0.48 | 0.21 | 0.71 |
| $^{68}$Ge-$^{68}$Ga | 271 d | 1.90 | 0.84 | 0.93 |

**(ii) Spin polarization of positrons from radioisotopes**

Energy (velocity) of positron emitted from radioisotope is determined by the $Q$ value, which is the excess energy of the whole decay process. This excess energy is distributed to the excitation of nucleus, and kinetic energies of positron and electron neutrino, giving rise to a continuous energy distribution of positron, $N(E)$, from zero to energy endpoint, $E_{max}$. Normally nuclear spin is random and hence positrons are emitted into $4\pi$ direction. Capturing positrons in a cone angle $\theta$, the energy- and $\theta$-averaged spin-polarization is given by

$$\langle P_+ \rangle = \frac{\langle v \rangle}{c}\frac{1+\cos\theta}{2} = \int_{E_1}^{E_2}\sqrt{1-\frac{1}{[1+E/(mc^2)]^2}}N(E)dE\,\frac{1+\cos\theta}{2} \qquad (1)$$

with an appropriate energy window ($E_1$ and $E_2$). Table 1 lists representative positron sources with their half-lives, energy endpoints, mean energies and helicities of positron [15]. For example, the energy-averaged spin polarization for $^{22}$Na is 72%. This further decreases to 36% with $\theta=\pi/2$, i.e., collecting positrons emitted into forward direction. In $^{68}$Ge-$^{22}$Ga, these are 93% and 47%, respectively. Thus, to obtain higher spin polarization, it is essential to use radioisotopes with higher energy endpoint, selecting higher energy components in a limited cone angle and align nuclear spins. The effect of energy selection will be discussed concerning spin polarization after moderation in sub-section (iii)-B. Method to determine spin polarization will be detailed in sub-section (iv)-C.

**(iii) Change of positron spin polarization in various processes**

**A. Depolarization in slowing-down and diffusion:** Positrons implanted into medium lose the kinetic energy to be thermalized via elementary excitations within ~10 ps. The Bremsstrahlung, of which the stopping power is proportional to $EZ/800$, may be less important in the energy region of radioisotopes. Major part of positron energy will be lost via the electromagnetic Bhabha scattering with ionization [16]. The spin-flipping probability in the Bhabha scattering was calculated as a function of positron energy in relatively high energy region [17]. With this calculation result for positron energy of ~0.5 MeV, and assuming appropriate energy loss per scattering, for example, 500 eV for tungsten, the spin-flipping probability may be of the order of $10^{-4}$. Further assuming 1000 times scatterings until total energy loss, approximately 10% depolarization may be expected. The depolarization probabilities accompanying the Mott scattering were calculated for electron in both elastic and inelastic scatterings [18]. If the calculation for electron is somehow applicable to positron and inelastic scattering is considered, the depolarization is likely less than 1%. Consequently, the net depolarization during the slowing-down is estimated to be 10 % at most. In the above arguments, the

depolarization during dielectric (e-h pairs and plasmons) and phonon excitations, that will occur in the energy range from eV to keV, were not considered.

After thermalization, positrons diffuse in medium until annihilation. Spin (Larmor) precession and thereby depolarization may occur due to both external and internal magnetic fields. This is especially important in ferromagnets. Even in paramagnets where spontaneous field is absent, depolarization may also occur due to influence of time-fluctuating electron spins. Positron spin relaxation [9] is argued on the analogy of muon spin relaxation (rotation) [19]. Unfortunately, positron spin relaxation process is hardly observed in the current time resolution of lifetime spectroscopy. If the time resolution is improved to be ~10 ps or less, positron spin relaxation process will be directly observed in age-momentum correlation spectroscopy enabling the trace of magnetic field along the positron pass.

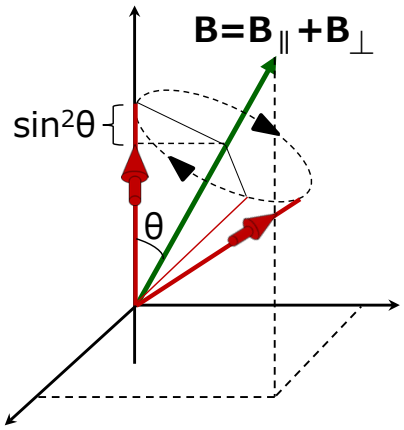


**Fig. 2** Head-swinging motion of spin in magnetic field.

In transverse magnetic field $B_\perp$ with respect to the positron spin polarization, positron spin rotates with angular frequency of $\omega = \gamma B_\perp$, where $\gamma$ is the gyromagnetic ratio, $\gamma = 1.761\text{x}10^{11}$ rad/s/T. It takes 89 ps per $\pi/2$ rotation in $B_\perp$=0.1 T, where longitudinal spin polarization is fully lost. Transverse relaxation, which is also called spin-spin or phase relaxation, also proceeds if the field is non-uniform. Since Zeeman splitting energy ($\Delta E=\hbar\gamma B$) is very small, e.g., ~0.1 meV even in $B$=1 T, initial spin polarization in longitudinal field $B_\parallel$, which is parallel to positron spin polarization, is eventually lost at finite temperatures. Under both longitudinal and transverse fields, positron spin undergoes head-swinging motion around the synthetic vector of $B_\parallel$ and $B_\perp$ with $\omega=\gamma(B_\parallel^2+B_\perp^2)^{1/2}$ as shown in Fig. 2. Time-dependent spin polarization is given by

$$P_+(t) = P_+(0)[\cos^2\theta + \sin^2\theta\cos(\omega t)], \tag{2}$$

where $\cos^2\theta=B_\parallel^2/(B_\parallel^2+B_\perp^2)$ and $\sin^2\theta=B_\perp^2/(B_\parallel^2+B_\perp^2)$. As known in nuclear magnetic resonance (NMR) theory, time-fluctuation of $B_\perp$ further induces longitudinal spin relaxation [9,20]. The relaxation function, which is the time-dependent spin polarization, is given by

$$G_z(t) = \exp(-t/T_1), \tag{3}$$

$$1/T_1 = (\gamma B_{dip,\perp})^2 \frac{\tau_c}{1+\tau_c^2\omega^2}, \tag{4}$$

where $\tau_c$ denotes the correlation time (roughly speaking, time scale of fluctuation) and $\omega_\parallel=\gamma B_\parallel$. For $\tau_c=1/\omega_\parallel$, $1/T_1$ takes maximum.

Ordinary SP-PAS measurement discussed in subsection (iv)-A is conducted with longitudinally spin-polarized positrons in external field parallel to positron spin polarization. Effective magnetic field is given by

$$\boldsymbol{B}_{eff} = \boldsymbol{B}_{ext} + \boldsymbol{B}_{demag} + \boldsymbol{B}_{Lorentz} + \boldsymbol{B}_{hf} + \boldsymbol{B}_{dip}, \tag{5}$$

where individual components in the right hand side are external, demagnetization, Lorentz, hyperfine and dipole fields, respectively. $\boldsymbol{B}_{demag}$, $\boldsymbol{B}_{Lorentz}$ and $\boldsymbol{B}_{hf}$ are parallel to $\boldsymbol{B}_{ext}$. Demagnetization and Lorentz fields are given by $\boldsymbol{B}_{demag}=-N\boldsymbol{M}$ and $\boldsymbol{B}_{Lorentz}=4\pi\boldsymbol{M}/3$, respectively, where $N$ is sample shape-dependent factor and $\boldsymbol{M}$ is the magnetization. The exact form of hyperfine field for positron has not yet been determined theoretically. On the analogy of muon spin relaxation, it may be written as $B_{hf}=(8\pi\mu_B/3)\int\left[n_-^{\downarrow}(\boldsymbol{r})-n_-^{\uparrow}(\boldsymbol{r})\right]n_+(\boldsymbol{r})\gamma_e[n_-(\boldsymbol{r})]d\boldsymbol{r}$ in cgs unit, where $\mu_B$ is the magnetic moment of electron, $n_-^{\downarrow}(\boldsymbol{r})$, $n_-^{\uparrow}(\boldsymbol{r})$ and $n_+(\boldsymbol{r})$ are the densities of majority and minority spin electrons, and positron, respectively, and $\gamma_e[n_-(\boldsymbol{r})]$ is the enhancement factor. If this is valid, then, the sign of $B_{hf}$ for positron is positive in many cases, because it is same as the sign of difference in annihilation rates between spin-up/down positrons given by Eq. (15). That is, the annihilation rate of spin-up positron is normally larger than that of spin-down positron reflecting that the number of majority spin electrons is more than that of minority spin electrons. Whereas, the sign of $B_{hf}$ for muon is negative in many cases because of the negative spin polarization at the interstitial sites where muon prefers to stay. Further studies, especially theoretical studies, are required to clarify the sign and magnitude of $B_{hf}$ for positron. $\boldsymbol{B}_{dip}$ generally has both parallel ($B_{dip,\parallel}$) and transverse ($B_{dip,\perp}$) components to $\boldsymbol{B}_{ext}$. Again, the theoretical form of $\boldsymbol{B}_{dip}$ for positron has not yet been established. On the analogy of muon, it may be written as the summation of all dipole fields created by the magnetic moment of $i$-th band electron, that are further space-averaged with positron density. In muon spin relaxation, it is thought that $B_{dip}$ vanishes in FCC metals because of cubic symmetry of interstitial sites where muon is located, while $B_{dip,\parallel}$ and $B_{dip,\perp}$ are finite in both BCC and HCT metals depending on crystal orientation with respect to external magnetic field [19]. However, these arguments may not be necessarily valid for positron because of the widely spread wave function in interstitial space, which is different from rather localized muon. To evaluate $\boldsymbol{B}_{dip}$ for positron, positron spin relaxation measurement should be carried out if it is possible, otherwise, we need to rely only on ab-initio calculation as once attempted [21]. Anyway, we have

$$B_{eff,\parallel}=B_{ext}+B_{demag}+B_{Lorentz}+B_{hf}+B_{dip,\parallel}, \tag{6}$$

$$B_{eff,\perp}=B_{dip,\perp}. \tag{7}$$

It is worth noting that the Stuttgart group pursued the effect of positron spin relaxation in ferromagnetic iron under the condition that a finite $B_{dip,\perp}$ was expected [9]. However, their results showed significantly small depolarization against initial expectation, implying much weaker $B_{dip,\perp}$ as compared to that determined in muon spin relaxation study. At present, again, we have no promising ways to predict depolarization amount during positron diffusion. We can only say that positron spin-polarization survives in some level as long as polarization effect is observed. Further studies are necessary.

**B: Spin polarization after moderation:** In the evaluation of survival spin polarization after moderation, before considering the above depolarization effect, the positron energy selection should be considered [22]. It may occur in (1) source material itself, (2) absorber and (3) moderator. The energy distribution of positrons emitted from the source may be given by

$$N_S(E)=(1/2)\int_0^{d_S}N_0(E)[A(z)/A_0]T_S(E,z)dz\,, \tag{8}$$

where $N_0(E)$ is the intrinsic energy distribution of radioisotope, $T(E, z)=\exp(-(z/z_0)^m)$ is the positron transmittance with $z_0=AE^n/[\rho\Gamma(1+1/m)]$, the density $\rho$ and $A$=4.0 mg cm$^{-2}$keV$^{-n}$, $A(z)/A_0$ is the source activity distribution with the normalization factor $A_0$, and $d_S$, is the source thicknesses.
Similarly, after the absorber with the thickness of $d_A$, the energy distribution is given by

$$N_A(E)=N_S(E)T_A(E,d_A). \tag{9}$$

Finally, the energy distribution of positrons that can be moderated in the moderator and emitted from the surface is given by

$$N(E) = N_S(E)T_A(E,d_A)\varepsilon_M(E,d_M)\,, \tag{10}$$

where $d_M$ is the moderator thickness and $\varepsilon_M(E,d_M)$ is the moderator efficiency, which is given by

$$\varepsilon_M(E,d_M) = P_{em}\int_0^{d_M} p(E,z)\sinh(z/L)\sinh(d_M/L)dz \tag{11}$$

for transmission type moderator and

$$\varepsilon_M(E,d_M) = P_{em}\int_0^{d_M} p(E,z)\exp(-z/L)dz \tag{12}$$

for reflection type moderator with branching ratio, $P_{em}$, positron implantation profile $p(E, z)$ and positron diffusion length, $L$ [23]. Positron spin polarization after moderation may be estimated with the energy distribution of Eq. (10) by multiplying the geometrical factor of $(1+\cos\theta)/2$ with $\theta=\pi/2$. For instance, assuming $^{22}$NaCl source with $d_S$=0.1 mm, transmission W moderator with $d_M$=1 μm and without absorber, the intrinsic spin polarization 36 % will be enhanced to 41 %.

Depolarization due to backscattered positrons in the source may be given by its coefficient, $R$=0.342log($Z$)–0.146 determined empirically [24]. For source tray made of carbon ($Z$=6), $R$ and therefore depolarization is approximately 10%. As mentioned in the sub-section (iii)-A, depolarization during slowing-down may be approximately 10%. Consequently, ultimate spin polarization of slow positron beam may be ~30% at most. Depolarization due to spin precession may be important in magnetic (re)moderators such as Ni. Relaxation function is simply given by $G_z(t)$=1/3+(2/3)cos($\omega t$) for random magnetic domain system and $G_z(t)$=cos($\omega t$) for homogeneously and transversely magnetized system. To estimate depolarization due to spin precession, the time spent in diffusion until emission and effective magnetic field for positrons should be known. Roughly speaking, approximately 10% depolarization is expected with 30 ps diffusion time and $B_\perp$=0.1 T.

**(iv) Spin-dependent positron annihilation**

**A. Bulk system:** SP-PAS measurement in magnetic field is conducted in longitudinal geometry, i.e., magnetic field and spin polarization are parallel/antiparallel. The spin-dependent positron annihilation was systematically modeled by Berko [25]. Here, the essence is summarized. Electron-positron momentum densities of majority (↓) and minority (↑) spin electrons with the band index $i$ are given by

**Table 2** Annihilation rates of spin up/down positron with electron in different spin states.

| | S=0 | S=1, $M_S$=0 | S=1, $M_S$=+1 |
|---|---|---|---|
| ↕ e⁺ | $\lambda_i^{\updownarrow 2\gamma}=\frac{1}{2}\lambda_S w_i^{\downarrow}$ | $\lambda_i^{\updownarrow 3\gamma}=\frac{1}{2}\lambda_T w_i^{\downarrow}$ | $\lambda_i^{\updownarrow 3\gamma}=\lambda_T w_i^{\uparrow}$ |
| | S=0 | S=1, $M_S$=0 | S=1, $M_S$=−1 |
| ↕ e⁺ | $\lambda_i^{\updownarrow 2\gamma}=\frac{1}{2}\lambda_S w_i^{\uparrow}$ | $\lambda_i^{\updownarrow 3\gamma}=\frac{1}{2}\lambda_T w_i^{\uparrow}$ | $\lambda_i^{\updownarrow 3\gamma}=\lambda_T w_i^{\downarrow}$ |

$$\rho_i^{\downarrow(\uparrow)}(\boldsymbol{p}) = \left|\int e^{-i\boldsymbol{p}\boldsymbol{r}}\Psi_+(\boldsymbol{r})\Psi_i^{\downarrow(\uparrow)}(\boldsymbol{r})\sqrt{\gamma_e(n_-(\boldsymbol{r}))}d\boldsymbol{r}\right|^2, \tag{13}$$

where $\Psi_+(\boldsymbol{r})$ and $\Psi_i(\boldsymbol{r})^{\downarrow(\uparrow)}$ are positron and electron wave functions, respectively. 1D-ACAR spectrum is given by $N_i^{\downarrow(\uparrow)}(p_z)=\iint\rho_i(\boldsymbol{p})^{\downarrow(\uparrow)}dp_xdp_y$. Overlap between positron and $i$-th band electron is given by

$$w_i^{\downarrow(\uparrow)} = \int_{-\infty}^{+\infty} N_i^{\downarrow(\uparrow)}(p_z)dp_z\,. \tag{14}$$

Annihilation rates between spin up/down positron (↟,↡) and electron are listed in Table 2, where $S$ and $M_S$ denote total spin and magnetic quantum number, respectively, $\lambda_S=4\pi r_e^2 c$ and $\lambda_T=\lambda_S/1115$. Total annihilation rates of spin up/down positron are

$$\lambda^{\updownarrow(\downdownarrows)} = \frac{1}{2}\sum_{i=1}^{occ.}\left[\lambda_S w_i^{\downarrow(\uparrow)} + \lambda_T(w_i^{\downarrow(\uparrow)} + 2w_i^{\uparrow(\downarrow)})\right], \tag{15}$$

where the summation goes over all occupied bands. 1D-ACAR spectra in positive and negative fields, and their difference and sum are given by

$$N_{+(-)}(p_z) = \frac{\lambda_S}{4}\sum_{i=1}^{occ.}\left[\frac{(1\pm P)N_i^{\downarrow}(p_z)}{\lambda^{\uparrow\!\!\uparrow}} + \frac{(1\mp P)N_i^{\uparrow}(p_z)}{\lambda^{\downarrow\!\!\downarrow}}\right], \tag{16}$$

$$\Delta N = N_+(p_z) - N_-(p_z) = \frac{\lambda_S P_+}{2}\sum_{i=1}^{occ.}\left[\frac{N_i^{\downarrow}(p_z)}{\lambda^{\uparrow\!\!\uparrow}} - \frac{N_i^{\uparrow}(p_z)}{\lambda^{\downarrow\!\!\downarrow}}\right], \tag{17}$$

$$\Sigma N = N_+(p_z) + N_-(p_z) = \frac{\lambda_S}{2}\sum_{i=1}^{occ.}\left[\frac{N_i^{\downarrow}(p_z)}{\lambda^{\uparrow\!\!\uparrow}} + \frac{N_i^{\uparrow}(p_z)}{\lambda^{\downarrow\!\!\downarrow}}\right], \tag{18}$$

respectively. Difference spectrum between majority and minority spin electrons is given by

$$\sum_{i=1}^{occ.}\left[N_i^{\downarrow}(p_z) - N_i^{\uparrow}(p_z)\right] = \frac{\lambda^{\uparrow\!\!\uparrow} + \lambda^{\downarrow\!\!\downarrow}}{\lambda_S P_+}\left[\Delta N + P_+\frac{\lambda^{\uparrow\!\!\uparrow} - \lambda^{\downarrow\!\!\downarrow}}{\lambda^{\uparrow\!\!\uparrow} + \lambda^{\downarrow\!\!\downarrow}}\Sigma N\right], \tag{19}$$

which may be physically more meaningful than Eq. (17) and comparable to magnetic Compton profile [26]. Thus, to get this difference spectrum, $\lambda^{\uparrow\!\!\uparrow(\downarrow\!\!\downarrow)}$ need to be determined in independent experiments. Approximating $\lambda^{\uparrow\!\!\uparrow(\downarrow\!\!\downarrow)} \sim \lambda_S w_i^{\downarrow(\uparrow)}/2$, mean positron lifetimes in positive and negative fields are given by

$$\lambda_{\pm} = \frac{1\pm P_+}{2}\lambda^{\uparrow\!\!\uparrow} + \frac{1\mp P_+}{2}\lambda^{\downarrow\!\!\downarrow}, \tag{20}$$

and thus $\lambda^{\uparrow\!\!\uparrow(\downarrow\!\!\downarrow)}$ may be determined with known $P_+$. Differences between $\lambda^{\uparrow\!\!\uparrow(\downarrow\!\!\downarrow)}$ predicted for Fe, Co and Ni are only 1.1, 0.3, 0.4 ns$^{-1}$, respectively [27,28]. Therefore, to determine $\lambda^{\uparrow\!\!\uparrow(\downarrow\!\!\downarrow)}$ experimentally, lifetime measurement system with high stability, sufficient time resolution (~100 ps or less) and tolerance to magnetic field need to be developed. The above formulas are general and applicable to both perfect bulk and vacancy systems.

**B. Surface system**: Surface spin-polarization of electrons is detected through the observation of positronium (Ps) annihilation fraction depending on the mutual direction between positron and electron spin polarizations [8]. Ps is characterized by $|S, M_S\rangle = |00\rangle$, $|10\rangle$, $|1{-}1\rangle$ and $|11\rangle$. The first one is called para and the rest three are called ortho. Apart from the details of electronic state, the fractions of individual Ps states are generally given by

$$F_{|00\rangle} = (1 - P_+P_-\cos\phi)/4, \tag{21}$$

$$F_{|10\rangle} = (1 - P_+P_-\cos\phi)/4, \tag{22}$$

$$F_{|11\rangle} = (1 + P_+ + P_-\cos\phi + P_+P_-\cos\phi)/4, \tag{23}$$

$$F_{|1-1\rangle} = (1 - P_+ - P_-\cos\phi + P_+P_-\cos\phi)/4, \tag{24}$$

where $\phi$ denotes the angle between positron and electron spin polarizations. Two-gamma and three-gamma fractions are given by

$$F_{Ps}{}^{2\gamma} = F_{|00\rangle}, \tag{25}$$

$$F_{Ps}{}^{3\gamma} = \varepsilon(1)(F_{|11\rangle} + F_{|1-1\rangle}) + \varepsilon(0)F_{|10\rangle}, \tag{26}$$

where $\varepsilon(M_S)$ denotes $M_S$-dependent detection efficiency [29]. Asymmetries of $F_{Ps}{}^{2\gamma}$ and $F_{Ps}{}^{3\gamma}$ on spin reversal are given by

$$A^{2\gamma} = \frac{F_{Ps}{}^{2\gamma}(+P_-) - F_{Ps}{}^{2\gamma}(-P_-)}{F_{Ps}{}^{2\gamma}(+P_-) + F_{Ps}{}^{2\gamma}(-P_-)} = P_+P_- \cos\phi\,, \tag{27}$$

$$A^{3\gamma} = \frac{F_{Ps}{}^{3\gamma}(+P_-) - F_{Ps}{}^{3\gamma}(-P_-)}{F_{Ps}{}^{3\gamma}(+P_-) + F_{Ps}{}^{3\gamma}(-P_-)} = \frac{2\varepsilon(1) - \varepsilon(0)}{2\varepsilon(1) + \varepsilon(0)} P_+P_- \cos\phi \,. \tag{28}$$

Here, $\pm P_-$ means parallel and antiparallel spin polarization of electrons with respect to spin polarization of positrons. Though asymmetry should exist both in two-gamma and three-gamma processes, in many cases, the former is difficult to be distinguished from free annihilation of positrons inside medium and/or the surface state. Hence, practically, three-gamma process is used for the determination of electron spin polarization. $F_{Ps}{}^{3\gamma}$ is determined as the intensity of 142 ns-component in lifetime spectrum ($F_{Ps}{}^{3\gamma}=I_{142\mathrm{ns}}$). While, in gamma-ray energy spectrum, it is determined from the intensity ($P$) of 511 keV photo peak and the intensity ($R$) below 511 keV as

$$F_{Ps}^{3\gamma} = \left[1 + \frac{P_{100\%}}{P_{0\%}} \frac{R_{100\%} - R}{R - R_{0\%}}\right]^{-1}, \tag{29}$$

where subscripts 0% and 100% denote Ps emission probabilities [30].

At solid surface, there are several Ps formation channels, such as direct emission with negative formation potential, surface-positron-mediated emission and dynamical neutralization of energetic positrons upon scattering. In the present discussion, the first one is relevant. Ps emission occurs when the formation potential is negative, i.e., $\varphi_{Ps}=\varphi_+ + \varphi_- - E_B<0$, where $\varphi_+$ and $\varphi_-$ are the positron and electron work functions, respectively, and $E_B$ is the Ps binding energy (=6.8 eV in vacuum). In the energy conservation, positrons can pick up electrons located at the energy level $E=E_F$ to $E=E_F+\varphi_{Ps}$, where $E_F$ is the Fermi level. The corresponding Ps energy is $E_{Ps}=-\varphi_{Ps}$ to zero. Furthermore, from the momentum conservation, pickable electron wave number parallel to the surface is limited to be $|k_{\parallel}| \le \sqrt{4m(E - E_F - \varphi_{Ps})}/\hbar$ . Therefore, in the practical Ps spectroscopy, the electron spin polarization $P_-$ in the above formulas should be replaced with $P_-(E)$ defined at $E_F+\varphi_{Ps} \le E \le E_F$ and $|k_{\parallel}| \le \sqrt{4m(E - E_F - \varphi_{Ps})}/\hbar$ , furthermore, taking into account of overlap between positron and electron densities (if more rigorously, evaluation of transition matrix should also be necessary). Defining such an electron-positron density of states, $D_{ep}(E)$, we may have

$$P_-(E) = \frac{D_{ep}^{\downarrow}(E) - D_{ep}^{\downarrow}(E)}{D_{ep}^{\downarrow}(E) + D_{ep}^{\downarrow}(E)}. \tag{30}$$

If Ps emitted into vacuum is simply observed without energy selection, an average $P_-$ in the energy range of $E_F+\varphi_{Ps} \le E \le E_F$ is obtained, and it is theoretically given by the energy-integral of Eq. (30). The experiment done by the Michigan group corresponds to this type [8]. In principle, negative spin polarization of Ni surface just below the Fermi level was not observed. If energy-resolved Ps spectroscopy is available, $P_-(E)$ is determined by the energy-dependent $A^{3\gamma}(E)$ of Eq. (28), and it is directly compared with theoretically calculated Eq. (30). This was demonstrated using spin-polarized Ps time-of-flight spectroscopy and negative spin polarization below the Fermi level of both Ni and Co has been confirmed [31].

**C. Ps annihilation in magnetic field for polarization measurement**: Magnetic quenching of Ps observed in media is useful in determining average spin polarization of positrons emitted from radioisotopes and also positron beam. Here, the fundamental formulas are summarized [32]. In magnetic field, |00> and |10> states are mixed and new states termed |00>' and |10>' are formed, while |11> and |1–1> states remain unchanged. Fractions of these new states are given by

$$F_{|00\rangle'} = \frac{(1-y)^2(1-P_+\cos\phi)(1+P_-)+(1+y)^2(1+P_+\cos\phi)(1-P_-)}{8(1+y^2)} \tag{31}$$

$$F_{|10\rangle'} = \frac{(1+y)^2(1-P_+\cos\phi)(1+P_-)+(1-y)^2(1+P_+\cos\phi)(1-P_-)}{8(1+y^2)}, \tag{32}$$

where $y = x/[\sqrt{1+x^2}+1]$ and $x = 4\mu_B B/\Delta E$ with the hyperfine interaction energy, $\Delta E$=8.4x10$^{-4}$ eV. Fractions for |11> and |1–1> states are given by Eqs. (23) and (24), respectively. Annihilation rates are given by

$$\lambda_{|00\rangle'} = \frac{\kappa\lambda_p}{1+y^2}+\frac{\kappa y^2\lambda_o}{1+y^2}+\lambda_{pick-off}, \tag{33}$$

$$\lambda_{|10\rangle'} = \frac{\kappa y^2\lambda_p}{1+y^2}+\frac{\kappa\lambda_o}{1+y^2}+\lambda_{pick-off}, \tag{34}$$

$$\lambda_{|11\rangle} = \lambda_{|1-1\rangle} = \kappa\lambda_o+\lambda_{pick-off}, \tag{35}$$

where $\lambda_o$ (0.0704 ns$^{-1}$) and $\lambda_p$ (8 ns$^{-1}$) are the intrinsic annihilation rates of ortho- and para-Ps, respectively, $\lambda_{pick\text{-}off}$ is pick-off annihilation rate and $\kappa$ is the contact density, $|\Psi_m(0)|^2/|\Psi_v(0)|^2$, where $\Psi_{m,v}$ denote the Ps wave functions in medium ($m$) and vacuum ($v$). $F_{Ps}{}^{2\gamma}$ and $F_{Ps}{}^{3\gamma}$ are given by

$$F_{Ps}{}^{2\gamma} = \frac{F_{|00\rangle'}}{\lambda_{|00\rangle'}}\left(\frac{\kappa\lambda_p}{1+y^2}+\lambda_{pick-off}\right)+\frac{F_{|10\rangle'}}{\lambda_{|10\rangle'}}\left(\frac{\kappa y^2\lambda_p}{1+y^2}+\lambda_{pick-off}\right)+\left(F_{|11\rangle}+F_{|1-1\rangle}\right)\frac{\lambda_{pick-off}}{\lambda_{|11\rangle}(=\lambda_{|1-1\rangle})}, \tag{36}$$

$$F_{Ps}{}^{3\gamma} = \frac{F_{|00\rangle'}}{\lambda_{|00\rangle'}}\frac{\kappa\lambda_o y^2}{1+y^2}+\frac{F_{|10\rangle'}}{\lambda_{|10\rangle'}}\frac{\kappa\lambda_o}{1+y^2}+F_{|11\rangle}\frac{\kappa\lambda_o}{\lambda_{|11\rangle}}+F_{|1-1\rangle}\frac{\kappa\lambda_o}{\lambda_{|1-1\rangle}}, \tag{37}$$

respectively. In the determination of spin polarization, the Michigan group observed three-gamma annihilation lifetimes of |10>', and |11> plus |1–1> of Ps formed in the pores of microchannel plate placed in magnetic field by rotating positron spin [6]. Using the second to fourth terms of Eq. (37) and assuming $P_-$=0, $\kappa$=1 and $\lambda_{pick\text{-}off}$=0, the three-gamma lifetime spectrum including annihilation events of unperturbed and perturbed ortho-Ps is given by

$$\begin{aligned}\frac{dN(t)}{dt} &\propto \left(F_{|11\rangle}\frac{\kappa\lambda_o}{\lambda_{|11\rangle}}+F_{|1-1\rangle}\frac{\kappa\lambda_o}{\lambda_{|1-1\rangle}}\right)\lambda_o\exp(-\lambda_o t)+\frac{F_{|10\rangle'}}{\lambda_{|10\rangle'}}\frac{\kappa\lambda_o}{1+y^2}\lambda_{|10\rangle'}\exp(-\lambda_{|10\rangle'}t)\\ &\propto 2\lambda_o\exp(-\lambda_o t)+\left(1-\cos\phi\frac{2yP_+}{1+y^2}\right)\lambda_{|10\rangle'}\exp(-\lambda_{|10\rangle'}t)\end{aligned}. \tag{38}$$

From the angular dependence of this intensity, $P_+$ is obtained. The Tokyo University group observed the field dependence of two-gamma annihilation of Ps by the Doppler broadening of annihilation radiation (DBAR) spectroscopy [33]. $S$-parameter is written as

$$\begin{aligned}S &= (S_{Ps}-S_{SiO_2})I(B)+S_{SiO_2}\\ &= (S_{Ps}-S_{SiO_2})\left(\frac{F_{|00\rangle'}}{\lambda_{|00\rangle'}}\frac{\kappa\lambda_p}{1+y^2}+\frac{F_{|10\rangle'}}{\lambda_{|10\rangle'}}\frac{\kappa y^2\lambda_p}{1+y^2}\right)+S_{SiO_2}\end{aligned}, \tag{39}$$

where $S_{Ps}$ is the $S$-parameter for |00>' plus |10>', $S_{SiO2}$ is the $S$-parameter for all the other two-gamma annihilation processes, and $I(B)$ is Eq. (36) with neglecting $\lambda_{pick\text{-}off}$. From the field dependence of $S$-parameter with known $\kappa$, $P_+$ is determined.

## Summary and Prospects

Spin-polarized positron annihilation spectroscopy may be a precious tool to study spin-related phenomena of solid materials concerning current spintronics. This owes to the natural spin polarization of source-based positrons, which is the gift of the parity non-conservation in the weak interaction. Position selectivity of this method would also be a remarkable feature. Using energy-tunable positron beams and conventional sources, electron spins at the first surface layer, buried interface in thin film layer, and in deep bulk region can be detected selectively. About detection of spins at atomic vacancies, there seems to be no potential and competitive methods.

In the study of bulk spin polarization, 2D-ACAR spectroscopy has been traditionally used concerning the Fermi surface mapping. DBAR and annihilation lifetime spectroscopies may also be used for detecting electron spins. Differences in annihilation lifetime and ACAR/DBAR spectrum between positive and negative magnetic fields are basically not much pronounced. Highly precise and stable measurements and also the further improvements of time and energy resolutions are required. As mentioned above, positron spin relaxation (rotation) spectroscopy abbreviated as $e^+$SR is currently not really practical as for the direct observation of time-dependent spin precession process. In this respect, development of lifetime measurement system with extremely high time resolution, i.e., less than 10 ps, is also an unavoidable element. Conversely, such a technological innovation will enable the observation of internal magnetic field by positron which may be different from that by muon.

In the study of surface spin polarization, the role of Ps spectroscopy may be very significant since Ps is formed only at the first surface layer except some special cases and hence obtained information is assured to be associated with the first surface layer. This may cover the drawback of photoemission spectroscopy. Although energy-resolved surface Ps spectroscopy has been developed so far for observing spin-polarized surface density of states [31,34], the further improvement to angle-resolved version is waited for to determine the spin-polarized band dispersions as well.

Lastly, it should be noted that to amplify spin-related signals in SP-PAS, positron spin-polarization should be as high as possible, ideally 100%, with less degradation of intensity. In this respect, the development of efficient positron filter may be an intriguing topic. Facility-based highly spin-polarized and intense positron source/beam is also strongly desired for the further advanced studies.

## References

[1] T. D. Lee, C. N. Yang, Phys. Rev. 104, 254(1956).

[2] C.S. Wu, E. Ambler, R. W. Hayward, D. D. Hoppes, R. P. Hudson, Phys. Rev. 105,1413 (1957).

[3] S. S. Hanna and R. S. Preston, Phys. Rev. 106,1363(1957).

[4] S. Berko and J. Zuckerman, Phys. Rev. Lett. 13,399(1964).

[5] P. E. Mijnarends and L. Hambro, Phys. Lett. 10,272 (1964).

[6] P. W. Zitzewitz, J. C. Van House, A. Rich and D. W. Gidley, Phys. Rev. Lett. 43,1281(1979).

[7] L. M. Liebermann, D. R. Fredkin and H. B. Shore, Phys. Rev. Lett. 22,539(1969).

[8] D. W. Gidley, A. R. Koymen and T. W. Capehart, Phys. Rev. Lett. 49,1779(1982).

[9] A. Seeger, J. Major, F. Banhart, Phys. Stat. Sol. (a) 102,91(1987).

[10] J. Puebla, J. Kim, K. Kondou, Y. Otani, Commun. Mater. 1, 24 (2020).

[11] F. Hellman et al., Rev. Mod. Phys. 89, 025006 (2017).

[12] Y. Ando, J. Phys. Soc. Jpn. 82, 102001 (2013).

[13] N. P. Armitage, E. J. Mele, A. Vishwanath, Rev. Mod. Phys. 90, 015001(2018).

[14] S. J. Gilbert, P. A. Dowben, J. Phys. D: Appl. Phys. 53, 343001 (2020).

[15] Nuclear Decay Data for Dosimetric Calculations, ICRP Publication 107, Annals of ICRP, 38(2008).

[16] F. Rohrich and B. C. Carlson, Phys. Rev. 93,38(1954).

[17] C. K. Iddings, G. L. Shaw and Y. S. Tsai, Phys. Rev. 135, B1388(1964).

[18] M. E. Rose and H. A. Bethe, Phys. Rev. 55,277(1938).

[19] A. Schenck, Muon Spin Rotation Spectroscopy, Adam Hilger Ltd, Bristol and London, 1985.

[20] J. Major, Spin-Polarized Positron Beam in Condensed-Matter Studies, in P. Coleman (Ed.), Positron Beams and their applications, World Scientific, New Jersey, London, Hog Kong, 1999, pp. 259-302.

[21] R. Blank, L. Schimmele and A. Seeger, in Positron Annihilation, L. Dorikens-Vanpraet, M. Dorikens, D. Segers (Eds.), World Scientific, Singapore, 1989, p. 278.

[22] M. Maekawa, Y. Fukaya, A. Yabuuchi, I. Mochizuki, A. Kawasuso, Nucl. Inst. Meth. Phys. Res. B 308, 9(2013).

[23] A. Vehanen, J. Mäikinen, Appl. Phys. A 36, 97(1985).

[24] I. K. MacKenzie, C. W. Shulte, T. Jackman, and J. L. Campbell, Phys. Rev. A 7, 135(1973).

[25] S. Berko, in Positron Annihilation, A. T. Stewart and L. O. Roellig (Eds.), Academic Press, New York, 1967, p. 61.

[26] N. Sakai and K. Ono, Phys. Rev. Lett., 37, 35(1976).

[27] H. Li, M. Maekawa, A. Kawasuso and N .Tanimura, J. Phys.: Condens. Matter 27, 246001 (2015) .

[28] J. Lin, T. Yamasaki and M. Saito, Jpn. J. Appl. Phys. 53, 053002 (2014)

[29] R. M. Drisko, Phys. Rev. 102, 1542(1956).

[30] S. Marder, V. W. Hughes, C. S. Wu, and W. Bennett, Phys. Rev. 103, 1258 (1956).

[31] M. Maekawa, A. Miyashita, S. Sakai, S. Li, S. Entani, A. Kawasuso and Y. Sakuraba, Phys. Rev. Lett. 126, 186401 (2021).

[32] Y. Nagashima and T. Hyodo, Phys. Rev. B41, 3937 (1990).

[33] Y. Nagai, Y. Nagashima, J. Kim, Y. Itoh, and T. Hyodo, Nucl. Instrum. Meth. Phys. Res. B 171,199 (2000).

[34] A. C. L. Jones, H. J. Rutbeck-Goldman, T. H. Hisakado, A. M. Piñeiro, H.W. K. Tom, and A. P. Mills, Jr., B. Barbiellini, J. Kuriplach, Phys. Rev. Lett. 117, 216402 (2016).